

Sevenless, a Cell-Specific Homeotic Gene of *Drosophila*, Encodes a Putative Transmembrane Receptor with a Tyrosine Kinase Domain

ERNST HAFEN, KONRAD BASLER, JAN-ERIK EDSTROEM, GERALD M. RUBIN

The determination of cell fates during the assembly of the ommatidia in the compound eye of *Drosophila* appears to be controlled by cell-cell interactions. In this process, the *sevenless* gene is essential for the development of a single type of photoreceptor cell. In the absence of proper *sevenless* function the cells that would normally become the R7 photoreceptors instead become nonneuronal cells. Previous morphological and genetic analysis has indicated that the product of the *sevenless* gene is involved in reading or interpreting the positional information that specifies this particular developmental pathway. The *sevenless* gene has now been isolated and characterized. The data indicate that *sevenless* encodes a transmembrane protein with a tyrosine kinase domain. This structural similarity between *sevenless* and certain hormone receptors suggests that similar mechanisms are involved in developmental decisions based on cell-cell interaction and physiological or developmental changes induced by diffusible factors.

THE NERVOUS SYSTEM IS A HIGHLY ORDERED STRUCTURE consisting of many cell types. Little is known about the genetic control underlying the generation of cellular diversity and specificity during neural development. Two very different but not exclusive mechanisms can account for the selection of distinct cellular pathways. First, cells may be programmed in a lineage-dependent manner by the asymmetric partitioning of determinants during cell division. Different developmental pathways are then selected in the daughter cells in response to the different localized determinants. Such cell-lineage dependent mechanisms may account for much of the development of the nematode *Caenorhabditis elegans* (1) and the mating type decision in the yeast *Saccharomyces cerevisiae* (2). Alternatively, cellular differentiation may occur in a lineage-independent manner where the position that a cell occupies in a developing field determines its fate. In this case, diffusible substances, such as hormones, or interactions with adjacent cells are the primary determinants of cellular differentiation. In many cases, a small group of cells, or even a single cell, selects a developmental program different from that of its neighbors. Because of the spatial specificity involved in such decisions, cues in the cell's local environment, such as a particular set of cellular contacts, most likely provide the required positional information, rather than long-range diffusible morphogens. Although the mechanisms used to read and interpret such positional information are largely unknown, short-

range cellular interactions are thought to be of principal importance in a wide variety of developmental phenomena including classical embryonic induction (3), regeneration (4), and the pathfinding of axon growth cones during neuronal development (5).

The compound eye of *Drosophila melanogaster* is an attractive system to study the mechanisms underlying lineage-independent developmental decisions since it consists of a small number of different cell types that develop in a lineage-independent manner (6–13). The compound eye consists of a two-dimensional array of approximately 800 ommatidia, or unit eyes. Each ommatidium contains 20 cells: eight photoreceptor cells, four cone cells that build the liquid-filled lumen underlying the lens, a sensory hair and nerve, and three types of pigment cells that optically insulate each ommatidium. The eight photoreceptor cells, which can be divided into three major classes (R1–R6, R7, and R8) based on morphology and spectral sensitivity, are arranged in a trapezoidal unit that is precisely repeated from ommatidium to ommatidium.

The compound eye develops from the eye imaginal disc during the third larval instar and pupal period (7, 9, 10, 13). Until the last larval instar, the eye imaginal disc consists of an epithelial monolayer of proliferating, undifferentiated cells. Over a period of approximately 2 days, the assembly of the ommatidial clusters proceeds in an orderly, progressive wave from the posterior to the anterior of the disc epithelium. Tightly associated with this process is a morphological depression, the morphogenetic furrow, that moves across the disc. Cells anterior to the furrow are undifferentiated; cells posterior to the furrow become assembled into the developing ommatidial clusters. The stereotyped assembly sequence and the precise conservation of the cellular contacts within each independently forming ommatidial unit indicate that cellular determination occurs in response to direct cellular contacts or to diffusible molecules with a range of only a few cell diameters (10). On the basis of these observations, Tomlinson and Ready have suggested that a cell's acquisition of a distinct identity depends on its contacts with neighboring cells in the assembling ommatidium that already express a given identity (10). For example, the information that would cue the R7 precursor for the R7 developmental pathway would be its particular combination of cell contacts with the already determined, adjacent R1, R6, and R8 precursor cells.

Attempts to isolate mutations that affect the R7 developmental pathway have been based on the fact that the R7 cell is the only

E. Hafen, K. Basler, and G. M. Rubin are in the Department of Biochemistry, University of California, Berkeley, CA 94720. J.-E. Edstroem is at the European Molecular Biology Laboratory, D-6900 Heidelberg, Federal Republic of Germany. The present address of E. Hafen and K. Basler is Zoologisches Institut, Universität Zürich, Winterthurerstrasse 190, 8057 Zürich, Switzerland. The present address of J.-E. Edstroem is Department of Genetics, University of Lund, 22362 Lund, Sweden.

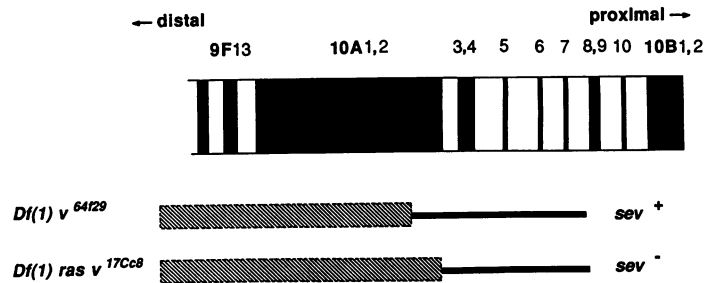


Fig. 1. A representation of the cytogenetic map of the 10 A-B region of the X chromosome is shown. The region shown constitutes approximately 2 percent of the X chromosome. The distal and proximal orientation of the chromosome with respect to the centromere is indicated. Black regions represent the cytological bands and white regions represent interband regions. The extent of chromosomal deletions that define the *sev* locus are shown below the chromosome map. The open hatched regions represent DNA removed in the deletions and the black bars represent DNA still present in the deleted chromosome. Only the proximal breakpoints of the deletions are shown; the distal breakpoints are located outside the region depicted. The *Df(1)v^{64f29}* in combination with a *sev* allele gives a *sev*⁺ phenotype, while *sev* in combination with *Df(1)ras v^{17Cc8}* is *sev*⁻. Therefore, at least part of the *sev* gene has to be located between the two deletion breakpoints at the proximal edge of the 10A1,2 band. Both of the deletions have been mapped cytologically by methods of electron microscopy (19). This very precise cytological localization of the *sev* gene made the microdissection cloning strategy feasible.

photoreceptor exclusively dedicated to reception of ultraviolet light. Thus, isolation of mutant strains that are impaired in ultraviolet light perception should provide mutations in genes that specifically affect either the development or function of the R7 cells. To date, such genetic screens have been carried out only for viable mutations located on the X chromosome, which constitutes about 20 percent of the genome of *Drosophila*, and a single genetic locus has been identified that appears to control the development of the R7 cell (14). Flies homozygous or hemizygous for any one of several *sevenless* (*sev*) mutant alleles specifically lack the R7 cell from each

ommatidium. Morphological studies suggested that in *sev*⁻ eye discs a cell occupies the normal position of the R7 precursor early in development of the photoreceptor cell cluster; however, this cell does not differentiate into a photoreceptor but into a nonneuronal cell, the cone cell (15). Thus, it appears that the *sev*⁺ gene is essential for the development of a single type of neuron, the photoreceptor cell R7; mutations in this gene result in the transformation of a photoreceptor cell into another cell type. Therefore, *sevenless* can be thought of as a cell type-specific homeotic mutation.

Selection of the R7 developmental pathway appears to be based

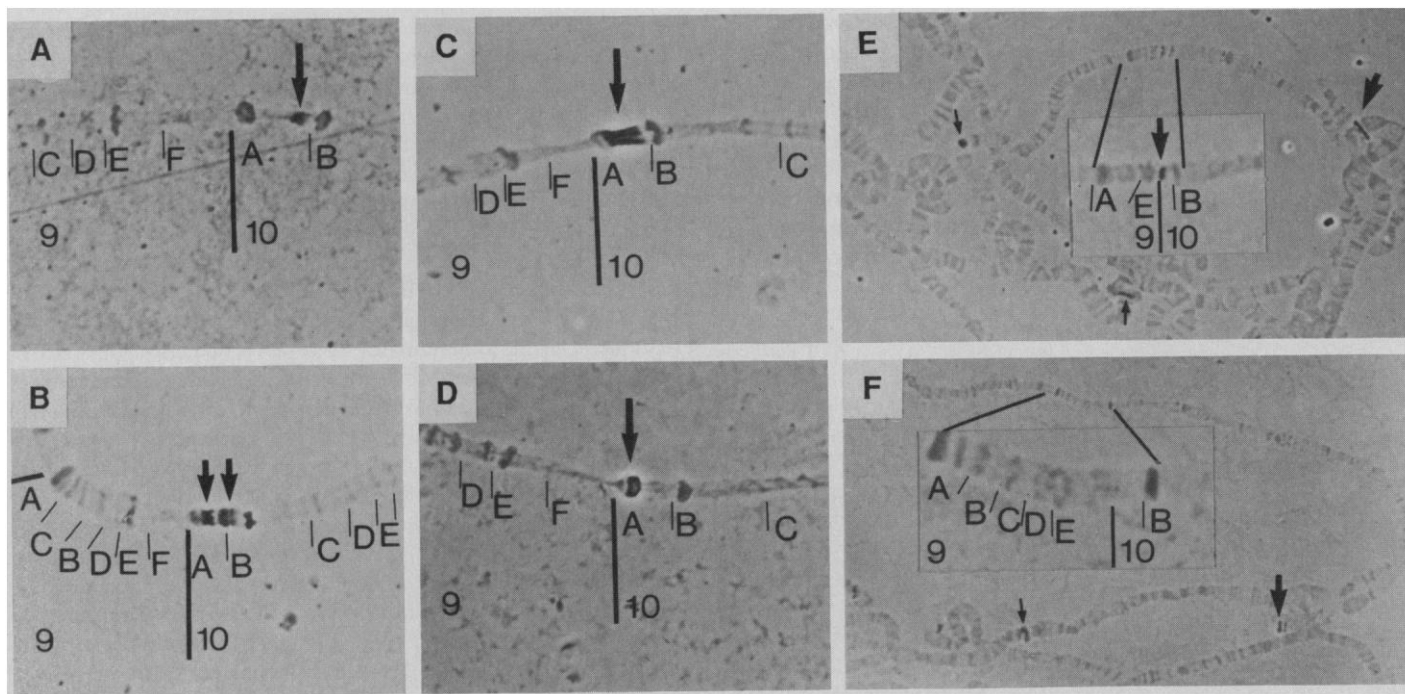
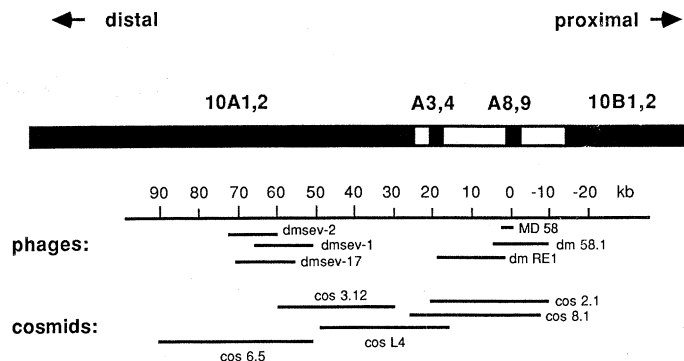


Fig. 2. Cytological representation of the chromosome walk and mapping of the *Df(1)v^{64f29}* breakpoint by in situ hybridization to polytene chromosomes. (A) The map position of the microdissected clone *MD 58* that was used as a starting point of the chromosome walk. The entire lambda recombinant containing a 2-kb insert of drosophila DNA was hybridized to polytene chromosome (22) squashes of Canton-S wild-type larvae. The arrow indicates the hybridization signal located in the interband region between 10A1,2 and 10B1,2. (B) The hybridization of a subclone containing fragments from the two ends of *cos 2.1*, a cosmid clone that was isolated by virtue of its homology to *MD 58*. These two fragments are separated by only 30 kb in the genome and yet give rise to two distinct hybridization signals. (C) Hybridization of the entire cosmid clone *cos LA*. The hybridization signal encompasses part of the interband and the proximal edge of 10A1,2. (D) The hybridization signal obtained with a 4-kb restriction endonuclease fragment from *amsev-1*, which is located in the *sev* region. The hybridization is to the proximal edge of the 10A1,2 band. (E and F) Mapping of cosmid clone *cos 6.5* to the *Df(1)v^{64f29}* chromosome. Male larvae

containing the *Df(1)v^{64f29}* and a translocation to the second chromosome of the X chromosomal region that is removed by the deletion where hybridized with subclones of *cos 6.5* that contain the restriction fragment from either the proximal or the distal end of cosmid. (E) Hybridization with the proximal fragment. Two major sites of hybridization are observed (large arrows). One site is to the translocated 10A region on the second chromosome and the other site is to the portion of the 10A1,2 band not removed by this deletion (inset). (F) Hybridization with the distal fragment of the *cos 6.5* clone. The only major site of hybridization observed is to the second chromosome; no signal is detected on the X chromosome (inset). This indicates that the distal end of the cloned region is deleted by *Df(1)v^{64f29}*. In addition to the major sites of hybridization due to the *cos 6.5* fragments two other sites of hybridization are observed with these probes (small arrows). These hybridization signals are due to the *cosPneo* vector, which contains fragments of the *white* gene on the X chromosome and from the major heat-shock gene *hsp70* on third chromosome.

Fig. 3. The extent of the cloned DNA in the 10A-B region of the X chromosome is shown. A simplified version of the cytological regional between 10A and 10B is depicted. The figure only includes the proximal edge of the 10A1,2 and the distal edge of the 10B1 bands. The extent of the various genomic clones used in the chromosome walk is shown. Distances from the starting point of the walk, the microdissected clone *MD 58*, are shown in kilobases. With the exception of the recombinant phage *dm RE1* which was isolated from a genomic library constructed from Canton-S flies in EMBL4 (51), all lambda clones were isolated from a genomic library of Canton-S DNA constructed in Charon-4 (21). The recombinant cosmid clones were isolated from libraries (21) constructed in the *cosPneo* cosmid vector. The relation between the clones was determined by hybridization within the group and in situ hybridization to chromosomes.



on the position that the R7 precursor occupies in the developing photoreceptor cell cluster, suggesting that the role of the *sev* product is either to provide the required positional information or to read these extracellular clues. Genetic analysis has distinguished these alternatives by showing that the mutant phenotype is cell autonomous, that is, the presence or absence of the R7 cell from the adult ommatidium appears to depend only on the genotype of the R7 precursor cell itself (16, 17). The *sev* gene must therefore be active in the R7 precursor cell to ensure proper R7 development, indicating that its product functions in reading or interpreting the positional information that elicits the R7 developmental pathway.

The analysis of the *sev* gene and its products should provide information on the molecular mechanisms involved in selection of a developmental pathway. Here we report the molecular cloning and analysis of the *sevenless* locus. Banerjee *et al.* have independently isolated the *sevenless* gene, by a different method (18). DNA sequence analysis of a complementary DNA (cDNA) clone suggests that *sev* encodes a membrane-spanning protein with a large extracellular domain and a cytoplasmic domain that exhibits a high degree of homology with the tyrosine kinase domains of a number of hormone receptors and proto-oncogene products. The structural features of the putative *sev* protein imply a direct role for *sevenless* in signal transduction in the developing eye and suggest a model for the mechanism of developmental decisions dependent on cellular interactions.

Isolation of the *sevenless* gene. The *sevenless* gene has been cytogenetically mapped to the 10A1,2 polytene band on the X chromosome (14, 19) (Fig. 1). We used the microdissection cloning

method (20) to obtain chromosomal DNA from the vicinity of the *sevenless* gene. In this technique the chromosomal region containing the desired gene is dissected from the polytene chromosomes present in the salivary glands of third instar larvae and used as a source of DNA for constructing a library in a bacteriophage lambda vector. Starting from a DNA segment obtained by microdissection cloning that mapped to the interband region between 10A1,2 and 10B1,2 (Fig. 2A) overlapping cloned DNA's were isolated from genomic DNA libraries constructed in bacteriophage lambda (21) and cosmid vectors (21). The positions of the cloned DNA's with respect to the chromosome map were determined by in situ hybridization to salivary gland chromosomes (22). This analysis was facilitated by the decondensed state of the chromosomal DNA in the interband region from which these DNA's originate (Fig. 2, B to D). For example, restriction fragments separated by only 30 kilobases (kb) mapped to opposite ends of the 10A-B interband region (Fig. 2B). Approximately 110 kb of chromosomal DNA derived from the interband between 10A1,2 and 10B1,2 and the proximal (with respect to the centromere) edge of 10A1,2 band were cloned. The extent of the different clones is shown in Fig. 3. Two overlapping chromosomal deletions define the position of the gene (19) (Fig. 1). The deletion *Df(1)v^{64f29}* removes part of the 10A1,2 band, but does not affect *sev* gene function. However, the deletion *Df(1)ras v^{17Cc8}*, which removes slightly more of the 10A1,2 band, results in a *sev⁻* phenotype. Therefore at least part of the *sevenless* gene is located between the breakpoints of these two deletions on the proximal side of the 10A1,2 band. DNA from the distal endpoint of the cloned region is deleted by the *Df(1)v^{64f29}* as

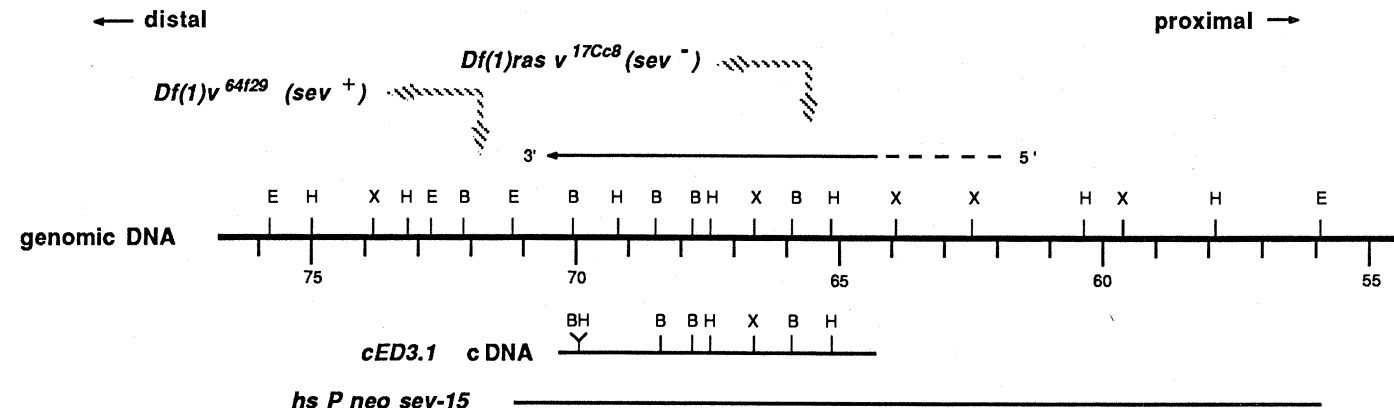


Fig. 4. A restriction map of the distal end of the cloned region. The heavy line represents 25 kb of genomic DNA encompassing the *sev* gene. Numbers below the line indicate the distance in kilobases from the start of the chromosome walk. Letters above the line represent restriction endonuclease sites. E, Eco RI; B, Bam HI; H, Hind III; X, Xho I. The cross-hatched arrows above the restriction map indicate the positions of the deletion breakpoints that define *sev* as determined by whole genome DNA blots (23).

The *Df(1)ras v^{17Cc8}* breakpoint has been mapped to a restriction fragment between 65.5 and 66.6 kb. The breakpoint for *Df(1)v^{64f29}* has been mapped between position 71.3 and 72.7 kb. The extents of the cDNA clone *ced3.1* and of the genomic fragment contained in *hsPneo-sev-15* are indicated below the line. The direction and approximate extent of the *sev* transcript are indicated by the arrow above the restriction map.

determined by in situ hybridization (Fig. 2, E and F). Since DNA deleted in the *Df(1)v^{64f29}* does not affect the *sev* gene, the chromosomal region that we isolated must extend distally beyond the *sev* gene (Fig. 1). A more precise mapping of the deletion breakpoints that define the distal boundary of the *sev* gene was obtained by hybridizing various cloned DNA segments from this chromosomal region to blots of restriction enzyme digests of DNA extracted from the two deletion strains (23). The results of this analysis are summarized in Fig. 4. The breakpoint of *Df(1)v^{64f29}* has been mapped to a restriction fragment at position 71.3 to 72.7 kb. The breakpoint of *Df(1)ras v^{17Cc8}*, which is associated with a *sev⁻* phenotype, has been mapped to between positions 65.5 and 66.6 kb. The genomic region located between these two breakpoints is approximately 7 kb in length and must contain at least part of the *sev* gene.

Rescue of the *sev* phenotype by germline transformation. To determine the extent of the *sev* gene within the cloned region, we

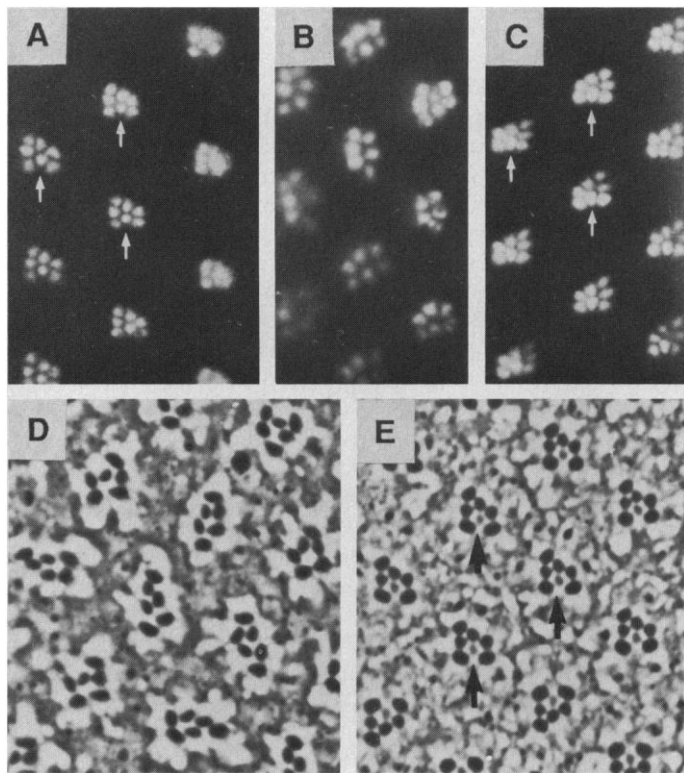


Fig. 5. Rescue of the *sev* mutant phenotype by germline transformation. (A to C) show the rhabdomere pattern of a wild-type fly, a *sev* fly, and a *sev*;P[*sev-15*, G418^r] fly by the optical neutralization technique (26). The white arrows indicate the R7 cell rhabdomere that is present in wild-type (A) and transformant (C) but not *sev* (B) flies. The different arrangement of the trapezoids in (A) and (C) is due to the fact that the photographs have been taken from different hemispheres of the eye, which exhibit a mirror image symmetry and is not an effect of *sev*. In (B) the mutant *sev* ommatidium at the top right shows seven instead of six rhabdomeres. Because of the vacant position of R7, the R8 cell can occasionally move up and occupy the R7 position (16). (D and E) Radial plastic sections through the distal portion of the retina of a *sev* fly and a *sev*;P[*sev-15*, G418^r] fly, respectively. The arrows in (E) point to the rhabdomere of the R7 cell; no R7 cell rhabdomeres are seen in the *sev* eye (D). The line of mirror image symmetry can be seen passing through the bottom third of (E). In sections through the distal region of the retina, no difference can be detected between the wild-type R7 cell and the R7 cell in the transformant. Serial sections through the entire depth of the retina, however, have indicated that the trapezoidal arrangement of the photoreceptors at the level of the R8 cell in the transformant is not as well conserved as in wild type. The reason for this difference is not known, since all the cells including the R7 cell occupy their correct positions. It is possible that the expression of the *sev* gene is not completely normal in this transformant line; the availability of more transformed lines is necessary to address this question.

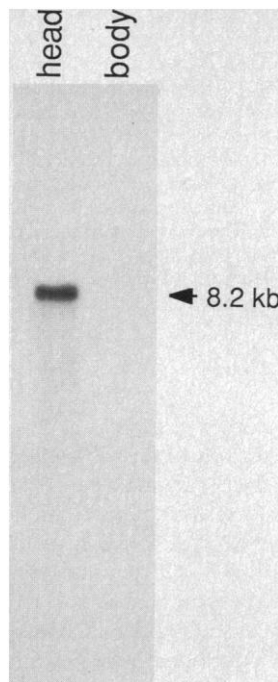


Fig. 6. An autoradiogram showing RNA blot analysis of the *sev* transcripts. Poly(A)⁺ RNA (4 μg) extracted from either adult heads or bodies was size-fractionated on an 0.8 percent agarose-formaldehyde gel, transferred to GeneScreen Plus (DuPont) and hybridized with single-stranded probes derived from the *cED3.1* cDNA clone (52). A single transcript of 8.2 kb is detected in heads but not in RNA extracted from bodies. The size of the RNA was estimated by comparison with RNA size markers (BRL RNA-ladder).

used P element-mediated germline transformation (24) to test the ability of a 15-kb genomic Eco RI DNA fragment (25) to complement the *sev* mutant phenotype. This fragment extends from 56 to 71 kb on the genomic map, includes the region between the deletion breakpoints, and extends proximally approximately 8 kb beyond the *Df(1)ras v^{17Cc8}* breakpoint (see Fig. 4). This fragment was inserted into the *pUChsneo* transformation vector that confers resistance to the drug G418 (21) to generate the construct *hsPneosev-15*, which was injected into wild-type embryos. The resulting adults were then crossed to *sev* flies, and the offspring were selected on food containing G418. One stably transformed line was obtained. A single insertion of the *hsPneosev-15* construct at 84C on the right arm of the third chromosome was detected in this line by in situ hybridization to polytene chromosomes of larvae resistant to G418.

Flies homozygous for *sev* and heterozygous for the *hsPneosev-15* insertion were examined for the presence of R7 cells. The presence or absence of the R7 cell can be detected in the intact eye with appropriate illumination (26) or by examining the arrangement of photoreceptor cells in histological sections of the adult retina. When the head is illuminated from the back, the rhabdomeres, the light-sensitive membranes of the photoreceptor cells, serve as light guides and reveal the regular arrangement of the photoreceptor cells in each ommatidium, a pattern referred to as the pseudopupil (26). In the wild-type eye the rhabdomeres of the outer photoreceptor cells (R1–R6) are arranged in an asymmetrical trapezoid (Fig. 5A). The R7 cell's rhabdomere is seen inside the trapezoid (arrow, Fig. 5A). The R8 rhabdomere resides below R7 and is not visible with this technique. In *sev* flies the absence of the R7 cell leads to a pseudopupil with only the six rhabdomeres of R1–R6 (Fig. 5B). The pseudopupil of a transformed fly is shown in Fig. 5C. The rhabdomere pattern of the transformant is indistinguishable from that of wild-type flies. Figure 5, D and E, shows tangential sections through the apical portion of the retina of a *sev* and transformant fly, respectively. The R7 cell is clearly visible in the transformed fly. Thus it appears that the fragment used for transformation is sufficient to complement the *sev* mutant phenotype, indicating that the *sevenless* gene is contained within this 15-kb DNA segment.

Expression of the *sev* gene. The cell autonomy of the *sev* phenotype leads to the expectation that the *sev* gene is expressed in

the developing eye disc. Indeed, hybridization of ^{32}P -labeled cDNA prepared from poly(A)⁺ RNA extracted from eye imaginal discs to DNA blots of representative phages and cosmids from the cloned region detected a transcribed region located within the 15-kb fragment that contains the *sevenless* gene. Restriction fragments from this region did not hybridize to cDNA probes derived from either wing disc RNA or tissue culture cell RNA suggesting that this region is selectively expressed in the eye disc. In order to characterize the *sev* transcript, we isolated several cDNA clones that were homologous to this chromosomal region (27). The longest of these cDNA clones, *cED3.1*, was 6.3 kb and its position on the genomic map is shown in Fig. 4. An RNA blot in which equal amounts of poly(A)⁺ RNA extracted from adult heads and bodies were hybridized with a single-stranded probe derived from *cED3.1* is shown in Fig. 6. One major transcript of 8.2 kb was detected in RNA extracted from adult heads, but not in RNA from bodies. A transcript of this size was also detected in poly(A)⁺ RNA extracted from total third instar imaginal discs. No transcript was seen, however, in RNA extracted from isolated wing discs or from whole organisms prior to the third larval instar. The direction of transcription as determined by hybridization with single-stranded probes is proximal to distal on the chromosome, or from right to left in Fig. 4.

To determine the spatial distribution of the *sev* transcripts, we examined the accumulation of the *sev* RNA's by in situ hybridization to tissue sections (28) of third instar larvae. A horizontal section of the anterior third of a wild-type third instar larva is shown in bright- and dark-field illumination in Fig. 7, A and B, respectively. This

section has been hybridized with a tritium-labeled genomic restriction fragment that is homologous to the 8.2-kb *sev* transcript. Specific accumulation of *sev* transcripts was observed over the bilaterally paired eye imaginal discs. No other site of hybridization was detected in the larva. A sagittal section of the central nervous system, including the eye disc, is shown in Fig. 7, C and D. Hybridization of the *sev* probe was observed over cells of the eye disc, but not in the brain or the ventral nervous system. Because of the ordered arrangements of the developing photoreceptor cell clusters in the third instar eye imaginal disc, the different stages of photoreceptor development are displayed spatially along the anterior to posterior axis of the disc. A higher magnification of a horizontal section through an eye disc is shown in Fig. 7, E and F. The silver grains were not uniformly distributed over the entire eye disc epithelium, but were localized apically over the posterior two-thirds of the disc epithelium. Cells in the anterior third of the disc did not contain significant levels of *sev* transcripts. The arrow in Fig. 7E indicates the position of the morphogenetic furrow. Cells anterior to the morphogenetic furrow are undifferentiated and randomly organized, whereas cells posterior to the furrow become selected to different developmental pathways and become organized into the ommatidial clusters. We detected *sev* transcripts around and posterior to the morphogenetic furrow. Therefore, it appears that the *sev* gene expression begins as soon as the developmental program for ommatidial assembly is initiated. The resolution of the in situ hybridization technique is not sufficient to determine precisely which ommatidial precursor cells express the *sev* gene. However, it appears that more cells than just the R7 precursors, which constitute

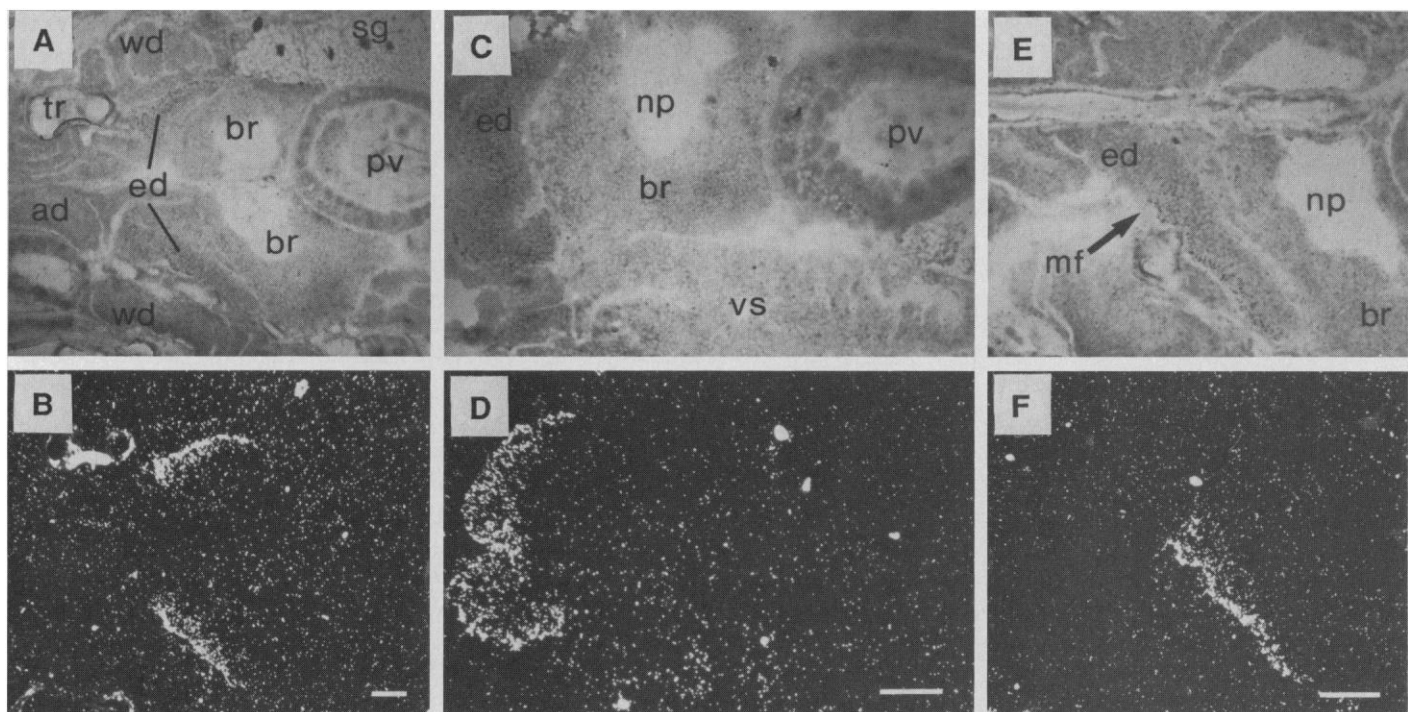


Fig. 7. Spatial distribution of *sev* transcripts in third instar larvae. Frozen tissue sections of wild-type third larvae were prepared as described (28) and hybridized with a 2.4-kb genomic Hind III restriction fragment derived from positions 65.2 to 67.6 on the genomic map that had been tritium labeled by nick translation. This probe is homologous to the 8.2-kb *sev* RNA detected on RNA blots. (A and B) Photomicrographs in bright- and dark-field illumination, respectively, of a horizontal section through the anterior third of a third instar larva. Specific accumulation of silver grains is detected over cells in the eye imaginal discs. No other tissue exhibits significant levels of hybridization. (C) (Bright-field) and (D) (dark-field) show a sagittal section through the central nervous system and the eye imaginal disc of a third instar larva. (E and F) Higher magnification of a horizontal section of

an eye disc. The different developmental stages of ommatidial development are spatially displayed along the posterior-anterior axis. The arrow indicates the position of the morphogenetic furrow. (While the furrow itself cannot be directly seen in these sections, its location can be inferred based on the position at which the axon bundle from the developing photoreceptor cells emerge from the basal side of the disc.) Specific hybridization is observed over a subpopulation of cells in the apical region of the disc epithelium immediately posterior to the morphogenetic furrow. Abbreviations: ad, antennal portion of the eye-antennal disc; br, brain; ed, eye imaginal disc; mf, morphogenetic furrow; np, neuropile; pv, proventriculus; sg, salivary gland; tr, trachea; wd, wing imaginal disc. The horizontal bars represent 100 μm . Anterior is to the left.

1.9 kb of the *sev* transcript, the open reading frame probably extends further upstream. Translation of the 6-kb open reading frame results in a polypeptide of 1993 amino acids. The predicted molecular size of the *sev* protein is therefore larger than 220 kD since *cED3.1* apparently does not include the entire coding region.

The hydrophobicity profile (30) of the *cED3.1* sequence reveals one stretch of 22 hydrophobic amino acids, which is long enough to span a membrane. The hydrophobicity index (30) of this putative transmembrane domain is 2.6; sequences with hydrophobicity indices greater than 1.6 are considered to have a high probability of being membrane spanning (30). The genetic analysis of the *sev*⁻ phenotype accommodates models predicting that the putative *sev* protein is located on the cell surface. Thus, if this hydrophobic stretch of amino acids is indeed used as a transmembrane domain, we might expect *sev* to encode a protein consisting of an extracellular domain in excess of 172 kD, a transmembrane sequence, and an intracellular domain of 45 kD.

Comparison of the deduced *sev* sequence with previously determined protein sequences (31) revealed a highly significant homology of the carboxyl terminal region of the putative *sev* protein with the tyrosine kinase domains encoded by several viral oncogenes and hormone receptors. The carboxyl terminal portion of the predicted protein sequence of the *sev* protein is shown in Fig. 8. This sequence is compared to the sequence of *c-ras* (32), the EGF receptor (33), and *v-src* (34). Shaded regions represent identities with the *sev* protein, and open boxes represent conservative amino acid substitutions. The strongest homology was found with *c-ras*, the cellular homolog of the oncogene *v-ras* of the chicken UR2 retrovirus (32). The putative *sev* protein shows 47 percent amino acid identity with *c-ras* over a stretch of 367 amino acids that includes the putative transmembrane and kinase domains. The highest degree of homology between *sev* and other proteins is found in a 65-amino acid section of the kinase domain; the putative *sev* and *c-ras* sequences share 56 identical and 4 conserved residues in this region. In addition to the high overall homology with other known tyrosine kinase domains, several residues that have been shown to be involved in specific aspects of the kinase activity are invariant. For example, the lysine at position 1681 in the *sev* protein is conserved in all kinases and has been shown to be involved in adenosine triphosphate binding (35, 36). The tyrosine at position 1821 in *sev* also is conserved. This residue has been shown to be the site of highest autophosphorylation in some tyrosine kinases (36).

A model for the function of the *sevenless* gene product. For the EGF and insulin receptors increased tyrosine phosphorylation is observed after the addition of the corresponding hormone (37, 38). These observations have led to the proposal that the tyrosine kinase acts as a mediator of signals received from the outside of the cell by phosphorylation of other cellular proteins (36). On the basis of the structural similarities of the putative *sev* protein with hormone receptors, we propose that the *sev* protein directly reads positional information specifying the R7 developmental pathway. In this model, the large extracellular domain of the protein would recognize the positional information that initiates R7 development. From what is known about eye development (9–11, 15–17), we anticipate that this information will be a unique combination of cellular contacts made by the R7 precursor with its neighbors in the assembling ommatidial cluster. In response to these cellular interactions, a signal would be transmitted into the cell by the action of the tyrosine kinase. If this hypothesis is correct (39), *sevenless* might define a new class of tyrosine kinase-containing receptors that interact with neighboring cells rather than diffusible factors.

If, as the above model predicts, *sevenless* mediates the primary signal in R7 cell determination, we would expect the *sev* protein to be present not only in precursors to R7 cells, but also in a larger

population of eye disc cells. However, its kinase would be activated only in the R7 precursor cell, since only this cell would receive the correct positional information. Consistent with this hypothesis, we believe that the number of eye disc cells that are labeled by in situ hybridization to *sev* transcripts is too large to consist just of the R7 precursor cells. A precise determination of the number and type of cells expressing the *sev* protein has to await the availability of specific antibodies that should provide the required histological resolution.

Many developmental decisions such as embryonic induction, axon guidance, and regeneration are thought to depend on similar cell-to-cell communication. The structural analogies between the *sevenless* protein and certain hormone receptors suggests that developmental pathway selections dependent on cell-cell interactions may involve similar molecular mechanisms to physiological or developmental changes induced by diffusible factors. Some hormones, such as the macrophage hormone CSF-1 (colony-stimulating factor) (40), share with *sev* the property of acting to promote differentiation of a small subpopulation of cells. However, hormone receptors respond to diffusible ligands and many such receptors induce proliferation in responding cells. In contrast, *sev* is active in postmitotic cells and is most likely activated by cell-cell interaction.

In *Drosophila*, a number of homeotic genes that control the differentiation of the body segments of the larva and adult have been identified (41). Molecular analysis of these homeotic genes has revealed the presence of a conserved protein domain that appears to be involved in DNA binding (41). These observations have led to the hypothesis that such homeotic genes control developmental pathways by directly binding to DNA, thereby altering gene expression and maintaining the stable inheritance of the determined state (41). In contrast, *sev* appears to alter developmental fate by mediating cellular communication and may only indirectly regulate gene expression. In both cases, however, mutation of the gene results in the homeotic transformation of the cells that normally depend on its function. In the case of *sev*, the R7 precursor develops into a cone cell, and in the case of the homeotic genes controlling segmentation one segmental structure is replaced by another.

As part of the effort to understand the role of cellular proto-oncogenes containing tyrosine kinase domains a number of *Drosophila* genes homologous to vertebrate oncogenes or hormone receptors have been isolated including *c-src* (42), the EGF receptor (43), and the insulin receptor (44). So far no mutations have been identified in any of these genes. Therefore, *sev* provides the first example of a genetically identified function for a cellular tyrosine kinase.

Our molecular analysis supports the model proposed for the assembly of the ommatidium (10) and encourages further genetic analysis of the R7 developmental pathway. The *sevenless* gene is the only gene that has been found in screens for nonlethal mutations affecting R7 cell development, although only one-fifth of the genome has been examined. The current working hypothesis for ommatidial assembly predicts the existence of additional components that might be identified by mutational analysis. For example, mutations in genes that encode the ligand recognized by the *sev* protein should also result in the absence of an R7 cell. However, in contrast to *sev*, such a mutation would not be cell autonomous, since the positional information is specified not by the R7 precursor but by its neighbors. In addition, the identification of other cell-autonomous mutations might define genes that act in the R7 precursor in response to the activation of the *sev* protein. In this way it might be possible to identify the substrates of the *sev* tyrosine kinase that are involved in transmitting the signal within the cell.

Three other genes involved in the selection of developmental pathways, *lin-12*, *Notch*, and *decapentaplegic*, encode products that show homology to proteins involved in hormonal regulation and

cellular communication. The *lin-12* gene, a cell-specific homeotic gene in the nematode *C. elegans* influences the development of a small number of cells that participate in vulval development (45). The *Notch* locus of *Drosophila* is required for the selection of ectodermal cells into the epidermal as opposed to the neurogenic pathway (46). The *decapentaplegic* gene complex is required for proper formation of dorsal structures in the developing *Drosophila* embryo and for proper morphogenesis of the imaginal discs (47). Its putative protein product shows homology to the members of the transforming growth factor- β (TGF- β) gene family (48). The products of both *Notch* and *lin-12* contain repeats of an EGF-like sequence similar to those found in the EGF precursor (49, 50), suggesting that these proteins could perform their functions by binding to specific receptors on other cells. Perhaps the positional cues that are recognized by the *sevenless* gene product are *Notch*-like or *lin-12*-like molecules on adjacent cells.

REFERENCES AND NOTES

- J. E. Sulston, E. Schierenberg, J. G. White, J. N. Thomson, *Dev. Biol.* **100**, 64 (1983); P. W. Sternberg and H. R. Horvitz, *Annu. Rev. Genet.* **18**, 489 (1984).
- J. N. Strathern and I. Herskowitz, *Cell* **17**, 371 (1979); I. Herskowitz, *Cold Spring Harbor Symp. Quant. Biol.* **50**, 565 (1986).
- J. Gurdon, *Cold Spring Harbor Symp. Quant. Biol.* **50**, 1 (1986).
- V. French, P. J. Bryant, S. V. Bryant, *Science* **193**, 969 (1976); L. Wolpert, *Curr. Top. Dev. Biol.* **6**, 183 (1971).
- C. S. Goodman *et al.*, *Science* **225**, 1271 (1984).
- O. Trujillo-Cenoz and J. Melamed, *J. Ultrastruct. Res.* **16**, 395 (1966).
- D. F. Ready, T. E. Hanson, S. Benzer, *Dev. Biol.* **53**, 217 (1976). Because of the progressive nature of eye development, each individual eye disc displays all the different stages of ommatidial development arranged along its posterior-to-anterior axis. The cells that become recruited to the ommatidial clusters arise from two final waves of mitotic activity that are closely associated with the morphogenetic furrow. The first mitotic wave generates the precursors for photoreceptor cells R8 and R2-R5, which form a five-cell precluster. All the other cell types, including precursors for R1, R6, and R7 photoreceptors arise in the second wave of mitoses immediately behind the morphogenetic furrow. The addition of R1 and R6, followed by R7, leads to the completion of the eight-cell cluster. The cellular identity of different photoreceptor cells is apparent from the position they occupy within the ommatidial cluster long before those cells become functional light receptors (9). Tomlinson and Ready (10), using antibodies to neural-specific antigens, have shown that photoreceptor cells start to express neural antigens in a precise sequence that most likely reflects the order in which they become integrated into the cluster.
- R. C. Hardie, in *Progress in Sensory Physiology*, D. Ottson, Ed. (Springer-Verlag, Berlin, 1984), vol. 5, pp. 1-79.
- A. Tomlinson, *J. Embryol. Exp. Morphol.* **89**, 313 (1985).
- and D. F. Ready, *Dev. Biol.* **120**, 366 (1987).
- P. A. Lawrence and S. M. Green, *ibid.* **71**, 142 (1979).
- J. C. Hall, *Q. Rev. Biophys.* **15**, 223 (1982).
- I. A. Meinertzhagen, in *Developmental Neurobiology of Arthropods*, D. Young, Ed. (Cambridge Univ. Press, New York, 1973).
- W. A. Harris, W. S. Stark, J. A. Walker, *J. Physiol. (London)* **256**, 415 (1976); G. F. Gereshheim, thesis, Ludwig-Maximilians-Universität, Munich (1981).
- A. Tomlinson and D. F. Ready, *Science* **231**, 400 (1986).
- J. A. Campos-Ortega, G. Jürgens, A. Hofbauer, *Arch. Entwicklungsmech. Org.* **186**, 27 (1979).
- A. Tomlinson and D. F. Ready, *Dev. Biol.*, in press. We thank these authors for giving us permission to cite their data prior to publication.
- Ü. Banerjee, P. J. Renfranz, J. A. Pollock, S. Benzer, *Cell*, in press.
- I. F. Zhimulev, V. F. Semeshin, E. S. Belyaeva, *Chromosoma* **82**, 9 (1981); I. F. Zhimulev, G. V. Pokholkova, A. V. Bgatov, V. F. Semeshin, E. S. Belyaeva, *ibid.*, p. 25.
- F. Scalenge, E. Turco, V. Pirrotta, M. Melli, J.-E. Edstroem, *ibid.*, p. 205; V. Pirrotta, H. Jäckle, J. E. Edstroem, in *Genetic Engineering, Principles and Methods*, A. Hollaender and S. K. Setlow, Eds. (Plenum, New York, 1983), vol. 5, pp. 1-17. Squashes of salivary gland chromosomes were prepared on cover slips. A chromosomal region containing the proximal part of 10A1,2 and the interband region to 10B1,2 was dissected from three individual X chromosomes. The DNA was extracted, digested with Eco RI restriction endonuclease, and cloned into lambda 641 cloning vector [N. E. Murray, W. J. Brammar, K. Murray, *Mol. Gen. Genet.* **150**, 53 (1977)]. Of the 100 individual microdissected clones obtained, 30 were chosen for further analysis since they contained *Drosophila* DNA inserts larger than 1 kb. The cytological locations of these 30 microdissected clones were then determined by *in situ* hybridization to salivary gland chromosomes. None of these clones mapped between the *Df(1)v⁶⁴²⁹* and *Df(1)ras v^{17C8}* breakpoints.
- The bacteriophage library was that described by T. Maniatis *et al.* [*Cell* **15**, 687 (1978)]. Two cosmid libraries, both made in the *cosPneo* vector [H. Steller and V. Pirrotta, *EMBO J.* **4**, 167 (1985)], were used. The recombinant cosmid clones *cos 2.1* and *cos 1.4* were from a library provided by E. Frei and M. Noll. Clones *3.12* and *cos 6.5* were from a library provided by H. Steller.
- P. R. Langer-Sofer, M. Levine, D. C. Ward, *Proc. Natl. Acad. Sci. U.S.A.* **79**, 4381 (1982). The described procedure was modified with the use of bio-16dUTP (ENZO Biochem) in the nick-translation reaction. Signal detection was achieved with streptavidin-conjugated horseradish peroxidase followed by histochemical detection with diaminobenzidine. These reagents were purchased as a signal detection kit (*DETEK-brp*) from ENZO Biochem.
- The chromosomal deletions *Df(1)v⁶⁴²⁹* and *Df(1)ras v^{17C8}* that were used to cytologically define the position of the *sev* gene include a number of lethal loci and are therefore homozygous lethal. The mapping of the deletion breakpoints by whole genome DNA blot analysis was carried out with DNA extracted from flies heterozygous for the corresponding deletion. As a control, DNA was extracted from flies hemizygous or homozygous for the corresponding balancer chromosome. For mapping *Df(1)v⁶⁴²⁹*, DNA was extracted from *Df(1)v⁶⁴²⁹/EM6* females, and *EM6* males were used as controls. For mapping *Df(1)ras v^{17C8}*, we used *Df(1)ras v^{17C8}/ct oc* females and *ct oc/ct oc* female control flies. The DNA was digested with restriction endonucleases, size-fractionated by agarose gel electrophoresis, and blotted to nitrocellulose. The blots were probed with recombinant genomic lambda clones from the appropriate chromosomal region. If a deletion breakpoint is in the DNA encompassed by the probe, restriction fragments included in the deletion would be present only in one copy (on the balancer chromosome) and would be revealed by the fact that they yielded signals only half as intense when compared with fragments in the same gel lane that fall outside the deletion. Often a novel restriction band could be detected that was not present in the control lane; such fragments most likely correspond to the new fragment created at the deletion breakpoint. For a reliable analysis it proved to be essential to use hybridization probes that cover a large region of the genomic DNA around the breakpoint. This permitted the comparison of the intensity of a number of fragments inside and outside the deletion and aided the identification of fragments which were only present in one copy. The breakpoint for the *Df(1)v⁶⁴²⁹* has been mapped to the 1.4-kb Eco RI fragment between 71.3 and 72.7 kb of the chromosome walk. The 15-kb Eco RI fragment proximal to the breakpoints was present in two copies, whereas the flanking 1.4-kb Eco RI fragment and the more distally located fragments were present in only one copy. Furthermore, in the Hind III digest fragments up the Hind III site at 69.2 kb were present in two copies but the flanking 4.0-kb fragment (between 69.2 and 73.3 kb) was only present in one copy, and a novel fragment of 6.0 kb appeared. The breakpoint for the *Df(1)ras v^{17C8}* has been mapped between that Hind III site at position 65.2 kb and a Sac I site at position 66.3 kb (not indicated in Fig. 4). The Hind III fragments up to the site at 65.2 kb were present in two copies, the flanking 2.3-kb fragment (65.2 to 67.5) and the more distally located fragments were present only in one copy. In the Sac I digest, the first fragment with half the intensity of the fragments present on both chromosomes was a 1.8-kb fragment between 64.5 and 66.3 kb. In the Sac I digest a novel fragment of 6.1 kb appeared, which most likely corresponds to the breakpoint fragment.
- A. C. Spradling and G. M. Rubin, *Science* **218**, 341 (1982); G. M. Rubin and A. C. Spradling, *ibid.*, p. 348.
- The 15-kb genomic Eco RI fragment used in the transformation experiments was isolated by construction and screening of a genomic library of size-selected 12- to 17-kb Eco RI fragments inserted into the EMBL4 [A. M. Frischauf, H. Lehrach, A. Poustka, N. Murray, *J. Mol. Biol.* **170**, 827 (1983)] phage vector. The cloned 15-kb Eco RI fragment was then subcloned into the *hsPneo* transformation vector [H. Steller and V. Pirrotta, in (21)].
- N. Franceschini, in *Photoreceptor Optics*, A. W. Snyder and R. Menzel, Eds. (Springer-Verlag, Berlin, 1975).
- The cDNA libraries that we screened were constructed by A. Cowman or H. Steller (unpublished data) in the λ gt10 vector [T. V. Huynh, R. A. Young, R. W. Davis, in *DNA Cloning I: A Practical Approach*, D. M. Glover, Ed. (IRL Press, Oxford, 1985)] with RNA from either mass-isolated third instar larval discs (gift of J. Fristrom) or eye discs that had been hand sorted from them.
- E. Hafen, M. Levine, R. L. Garber, W. J. Gehring, *EMBO J.* **2**, 617 (1983).
- F. Sanger, S. Nicklen, A. R. Coulson, *Proc. Natl. Acad. Sci. U.S.A.* **74**, 5463 (1977). The nucleotide sequence of the *cED3.1* cDNA was determined by sequencing fragments that had been randomly shared by sonication and cloned in the M13mp8 vector. The assembly and analysis of the sequence was performed with the use of Intelligenetics Inc. software. The complete sequence of both strands was determined. Several clones that contained GC-rich regions were sequenced again with 7-deaza-dGTP [S. Mizusawa *et al.*, *Nucleic Acids Res.* **14**, 1319 (1986)] to avoid compression artifacts due to secondary structure.
- J. Kyte and R. F. Doolittle, *J. Mol. Biol.* **157**, 105 (1982).
- D. J. Lipman and W. R. Pearson, *Science* **227**, 1435 (1985).
- W. S. Neckameyer, M. Shibuya, M. Hsu, L. Wang, *Mol. Cell. Biol.* **6**, 1478 (1986).
- A. Ullrich *et al.*, *Nature (London)* **309**, 418 (1984).
- D. E. Schartz, R. Tizard, W. Gilbert, *Cell* **32**, 853 (1983); A. P. Czernilofsky *et al.*, *Nature (London)* **301**, 736 (1983).
- M. J. Zoller, N. J. Nelson, S. S. Taylor, *J. Biol. Chem.* **256**, 10837 (1981); M. P. Kamps, S. S. Taylor, B. M. Sefton, *Nature (London)* **310**, 589 (1984).
- T. Hunter and J. A. Cooper, *Annu. Rev. Biochem.* **54**, 897 (1985).
- G. L. Carpenter, S. King, S. Cohen, *Nature (London)* **276**, 409 (1978); H. Ushiro and S. Cohen, *J. Biol. Chem.* **255**, 8363 (1980).
- L. M. Petruzzelli *et al.*, *Proc. Natl. Acad. Sci. U.S.A.* **79**, 6792 (1982).
- We realize that it is formally possible that the R7 precursor cell could be predisposed to receive a signal from a long-range diffusible factor. However, this model leads to several conceptual difficulties. For example, how does the R7 precursor get to this state? On the basis of morphological and genetic data (9, 10, 17) we do not favor this model. However, it is not possible from the available data to distinguish between direct cell-cell contact and a diffusible factor with a range of only a few cell diameters. Final resolution of these issues depends on identifying the putative ligand.
- The macrophage hormone CSF-1 stimulates hematopoietic precursor cells to form colonies containing mononuclear phagocytes. Unlike the granulocyte-macrophage colony-stimulating factor and interleukin-3, which also directly induce mononuclear phagocyte proliferation, CSF-1 is lineage-specific and alone does not stimulate the proliferation of granulocytic or erythroid precursor cells [E. R. Stanley *et al.*, *J. Cell. Biochem.* **21**, 151 (1983)]. The receptor for CSF-1 is related and possibly identical with the protooncogene *c-fms* and contains a tyrosine kinase activity [C. Sherr *et al.*, *Cell* **41**, 665 (1985)].
- For reviews see: W. J. Gehring and Y. Hiromi, *Annu. Rev. Genet.* **20**, 147 (1986);

- M. P. Scott and P. H. O'Farrell, *Annu. Rev. Cell. Biol.* 2, 49 (1986).
42. M. A. Simon, B. Drees, T. Kornberg, J. M. Bishop, *Cell* 42, 831 (1985).
43. E. Livneh, L. Glazer, D. Segal, J. Schlessinger, B. Shilo, *ibid.* 40, 599 (1985); E. D. Schejter, D. Segal, L. Glazer, B. Shilo, *ibid.* 46, 1091 (1986).
44. L. Petruzzelli *et al.*, *Proc. Natl. Acad. Sci. U.S.A.* 83, 4710 (1986).
45. I. S. Greenwald, P. W. Sternberg, H. R. Horvitz, *Cell* 34, 435 (1983).
46. D. F. Poulson, *Proc. Natl. Acad. Sci. U.S.A.* 23, 133 (1937).
47. F. A. Spencer, F. M. Hoffman, W. M. Gelbart, *Cell* 28, 451 (1982); D. Segal and W. M. Gelbart, *Genetics* 109, 119 (1985).
48. R. W. Padgett, R. D. St. Johnston, W. M. Gelbart, *Nature (London)* 325, 81 (1987).
49. I. S. Greenwald, *Cell* 43, 583 (1985).
50. K. A. Wharton, K. M. Johanson, T. Xu, S. Artavanis-Tsakonas, *ibid.*, p. 567.
51. Gift of V. Pirrotta. The EMBL4 vector is described in A. M. Frischhaut, H. Lehrach, A. Poostka, N. Murray, *J. Mol. Biol.* 170, 827 (1983).
52. The single-stranded hybridization probe used for the RNA blot shown in Fig. 6 was a mixture of probes derived from five overlapping M13 clones from *cED3.1* cDNA that were used in the DNA sequence determination (29). These clones cover 3 kb at the 5' end of the cDNA. The same RNA blot was also hybridized with a single-stranded probe derived from five M13 clones from the 2 kb closest to the 3' end of the cDNA. Again the only major transcript detected was the 8.2-kb transcript.
53. Supported by NIH grant GM32795; an EMBO Long Term Fellowship (E.H.), the Janggen-Pöhn Stiftung (E.H.), and Kanton Zürich (K.B.). We thank Tulle Hazelrigg for transporting chromosome squashes from Berkeley to Heidelberg on her way to Greece and our many colleagues for advice and comments on the manuscript.

3 February 1987; accepted 2 March 1987

